# Chapter 14
# Neural Field Modelling of the Electroencephalogram: Physiological Insights and Practical Applications

**David T. J. Liley**

**Abstract** The aim of this chapter is to outline a mean field approach to modelling brain activity that has been particularly successful in articulating the genesis of rhythmic electroencephalographic activity in the mammalian brain. In addition to being able to provide a physiologically consistent explanation for the genesis of the alpha rhythm, as well as expressing an array of complex dynamical phenomena that may be of relevance to understanding cognition, the model is also capable of accounting for many of the macroscopic electroencephalographic effects associated with anaesthetic action, a feature often missing in similar formulations. This chapter will then conclude with an example of how the physiological insights afforded by this mean field modelling approach can be translated into improved methods for the clinical monitoring of depth of anaesthesia.

## 14.1 Introduction

In recent years there has been a resurgence of interest in utilising the electroencephalogram (EEG) to understand brain function. While it was the first functional measure of brain function [1, 32], unlike the subsequently developed blood oxygen level dependent functional magnetic resonance (fMRI) and radionuclide imaging techniques, it has generally been viewed as too coarse in its spatial field of view to reveal anything meaningful about the inner workings of the brain. However with the limitations of fMRI becoming all too apparent and recent advances in our understanding of the anatomical and physiological organization of cortex challenging simplistic views of cortex being just an axo-synaptically coupled network of neurons, EEG, together with its electromagnetic counterpart the

D.T.J. Liley (✉)
Brain and Psychological Sciences Research Centre, Swinburne University of Technology, P.O. Box 218, Hawthorn VIC 3122, Australia
e-mail: dliley@swin.edu.au

S. Coombes et al. (eds.), *Neural Fields*, DOI 10.1007/978-3-642-54593-1_14,

magnetoencephalogram (MEG), is re-emerging not only as an important functional measure of brain activity, but also as the basis about which physiologically meaningful mesoscopic formulations of cortical dynamics can be formulated [46].

The EEG is a sensitive measure of behavioural and cognitive state [53]. Spontaneous EEG reveals characteristic and systematic changes during sleep and anaesthesia [34], whereas time locked and/or averaged EEG, has been shown to be a sensitive indicator of cognitive performance and function [63]. In disease it can exhibit features of singular diagnostic importance – from spike and wave activity characteristic of epilepsy to the wicket rhythms pathognomonic for the transmissible spongiform encephalopathy known as Creutzfeldt-Jakob disease [55]. Nevertheless despite our detailed empirical knowledge regarding the patterns and features of EEG our understanding of the physiological genesis of such patterns is comparatively meagre.

While the biophysical origins of the EEG are relatively well established [57] the mechanisms responsible for its dynamical genesis, despite decades of investigation, remain uncertain. For example it was previously believed that the alpha rhythm, a characteristic waxing and waning oscillation of between 8 and 13 Hz, was restricted to the occipital lobe and was due to cortical tissue being driven by oscillatory activity arising from the thalamus [5] or to the existence of distributed subpopulations of pyramidal neurons having some form of intrinsic rhythmicity [47]. However we now believe that dynamical activity in the EEG *emerges* from a panoply of interactions between neuronal and non-neuronal cell populations in cortex [48]. How then do we theoretically instantiate such a view so that we can use it to explain existing electroencephalographic phenomena and make the predictions necessary for its ontological justification?

Two broad theoretical approaches declare themselves as frameworks for understanding the genesis of the EEG. The most obvious is to assume that cortex is a network of neurons and model the individual neurons and their interactions. Apart from the obvious problem of dealing with the computational tractability of simulating the hundreds of thousands of neurons, and their connections, that underly a typical scalp EEG electrode, is the issue of how much physiological detail to include and how to meaningfully parameterise it. We now know that the functional structure of cortex extends well beyond neurons and their axosynaptic interactions. Glial cells, originally thought to only provide structural and biochemical support to the neuronal parenchyma, have been shown to regulate neuronal activity through a "tripartite" synapse – a complex involving an astrocyte and the pre- and post-synaptic terminals of a pair of neurons [31]. Add to this the suggestions of new modes of neuronal interaction (e.g. the axo-myelenic synapse) [73], potential ephaptic (local field) [74] and diffusive (gap junction) neuronal coupling [69], volume (extrasynaptic) neurotransmission [23] and non-synaptic plasticity [52], let alone the known complexities of single neuronal function, then not only does a network motivated approach to understanding the EEG seem daunting, it comes with considerable uncertainties as to how much detail should be included.

A preferable approach then to articulating the genesis of the EEG will be one that (i) has spatiotemporal scales commensurate with EEG and ECoG (ii) is able to deal with the uncertainties of structural, and therefore functional, composition

of cortical tissue and (iii) handles the sparseness of neuronal firing [8] and the unreliability of neuronal interconnectivity that arise as a consequence of low in vivo synaptic release probabilities [12]. The framework of mean field modelling, in which interactions between individual elements are replaced by *effective* averages, has emerged as one powerful way to address these requirements while at the same time remaining physiologically and anatomically pertinent [22, 46].

Commencing with the pioneering works of Beurle [10], Freeman [26], Nunez [56], Wilson and Cowan [77, 78], and Amari [4], mean field models of the EEG have evolved from being relatively abstract biomathematical formulations to frameworks that will be central for the analysis, organization and integration of large volumes of high dimensional functional imaging data [21]. The aim of this chapter is to describe one mean field modelling approach that has been developed to account for electrorhythmogenesis of the mammalian EEG and to illustrate its relevance to understanding the modulation of cortical activity during health and disease.

## 14.2 A Mean Field Model of Electrocortical Rhythmogenesis

Despite the avowed advantages of a mean field approach over a network approach in understanding the genesis of rhythmic activity in the EEG, almost all mean field approaches take as their starting point the physiological and anatomical properties of axo-synaptically coupled networks of neurons. Commencing with the work of Beurle [10], in which cortex was modelled as a continuous network of spatially uniform, fixed firing threshold, excitatory neurons devoid of any membrane or synaptic dynamics, mean field models have evolved to include many of the most significant anatomical and physiological features immanent to cortical tissue. Of these models one of the more successful in generating dynamics consistent with that of human EEG is that of Liley et al. [11, 40–42]. This model differs from other well known mean-field formulations in (i) explicitly separating the synaptic kinetics of cortical excitatory and inhibitory neuronal activity (cf. [66]) (ii) not needing to explicitly model cortico-thalamic feedback in order to generate cortical rhythms (cf. [66]) (iii) separating out intracortical (short-range) and cortico-cortical (long range) fibre connectivity (cf. [37]) (iv) including the full panoply of local feedforward and feedback excitatory and inhibitory coupling (cf. [35]) and (vi) incorporating synaptic reversal potentials such that a conductance-based mean neuron (see below) is defined (cf. [35, 66, 76]).

In essence the model of Liley et al. [11, 40–42] is constructed at the scale of the cortical macrocolumn – an approximately barrel shaped region extending through the entire thickness of the cortical sheet that has a lateral extent within the cortical sheet of the order of the characteristic scale of pyramidal neuron recurrent collaterals. Within this column, extending across all cortical layers, are distributed populations of excitatory and inhibitory neurons interacting with each other by all possible feedforward and feedback axo-dendritic connections. Macrocolumns then interact with each other by the axons of the excitatory pyramidal neurons

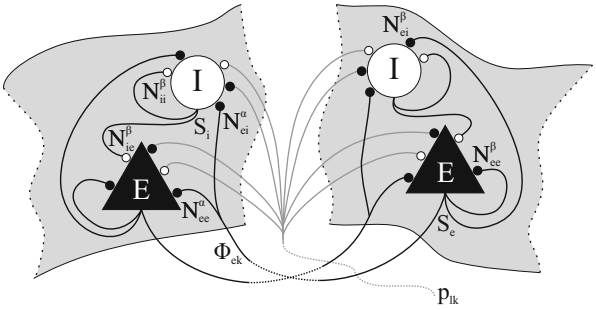


**Fig. 14.1** Model topology (Figure reproduced with permission from [25])

that pierce through the bottom layer of cortex to form the long range cortico-cortical conduction system. The topological organization of this model is well known and is depicted in Fig. 14.1 in which the interactions within and between two cortical macrocolumns are shown. In this model "equations-of-motion" for the soma membrane potentials of excitatory and inhibitory neurons, averaged over the spatial extent of the macrocolumn, are defined. Cortical activity is then described by the spatiotemporal evolution of these mean excitatory, $h_e$, and inhibitory, $h_i$, membrane potentials. The connection with electrophysiological experiment is through $h_e$, which is assumed to be linearly related to the EEG. Excitatory and inhibitory neurons are modelled as a single passive resistor-capacitor circuit in which all synaptically induced postsynaptic currents($I_{lk}$) flow. On this basis the following *conductance-based* mean neuron can be defined:

$$\tau_k \partial_t h_k = h_k^r - h_k(r,t) + \sum_{l=e,i} \frac{h_{lk}^{eq} - h_k(r,t)}{|h_{lk}^{eq} - h_k^r|} I_{lk}(r,t) \ , \tag{14.1}$$

where $r \in \mathbb{R}^2$ is position on the cortical sheet and double subscripts represent first source and then target.[1] Postsynaptic "currents" [2] ($I_{lk}$) are weighted by the ionic driving forces, which are defined to be unity at the resting membrane potential $h_k^r$ such that a unitary postsynaptic potential can be simply parameterised. The remaining parameters are defined in Table 14.1.

The dynamics of the postsynaptic "currents" ($I_{lk}$) are described by a critically damped oscillator driven by the mean rate (i.e. the *mean field*) of incoming excitatory or inhibitory axonal pulses, $A_{lk}$:

$$(\partial_t + \gamma_{lk})^2 I_{lk}(r,t) = e\gamma_{lk} \Gamma_{lk} \cdot A_{lk}(r,t) \tag{14.2}$$

[1] Where in contrast to other authors we have adopted a "anatomical" index ordering.

[2] We are being quite sloppy with our terminology here as these "currents" are more correctly identified as being conductances but have units of volts as a consequence of being weighted by ionic driving forces normalised to be unity at rest.

**Table 14.1** Liley model parameters (Table reproduced with permission from [45])

| | Definition | Min., Max. | Units |
|---|---|---|---|
| $h_k^r$ | Resting membrane potential | $-80,\ -60$ | mV |
| $\tau_k$ | Passive membrane decay time | $5,\ 150$ | ms |
| $h_{ek}^{\text{eq}}$ | Excitatory reversal potential | $-20,\ 10$ | mV |
| $h_{ik}^{\text{eq}}$ | Inhibitory reversal potential | $-90,\ h_k^r - 5$ | mV |
| $\Gamma_{ek}$ | EPSP peak amplitude | $0.1,\ 2.0$ | mV |
| $\Gamma_{ik}$ | IPSP peak amplitude | $0.1,\ 2.0$ | mV |
| $1/\gamma_{ek}$ | EPSP rise time to peak | $1,\ 10$ | ms |
| $1/\gamma_{ik}$ | IPSP rise time to peak | $2,\ 100$ | ms |
| $N_{ek}^{\alpha}$ | No. of excitatory cortico-cortical synapses | $k=e$: 2,000, 5,000<br>$k=i$: 1,000, 3,000 | – |
| $N_{ek}^{\beta}$ | No. of excitatory intracortical synapses | 2,000, 5,000 | – |
| $N_{ek}^{\beta}$ | No. of inhibitory intracortical synapses | 100, 1,000 | – |
| $v_{ek}$ | Axonal conduction velocity | $0.1,\ 1$ | $\frac{\text{mm}}{\text{ms}}$ |
| $1/\Lambda_{ek}$ | Decay scale of cortico-cortical connectivity | $10,\ 100$ | mm |
| $S_k^{\max}$ | Maximum firing rate | $0.05,\ 0.5$ | $\text{ms}^{-1}$ |
| $\mu_k$ | Firing threshold | $-55,\ -40$ | mV |
| $\sigma_k$ | Standard deviation of firing threshold | $2,\ 7$ | mV |
| $p_{ek}$ | Extracortical synaptic input rate | $0,\ 10$ | $\text{ms}^{-1}$ |

In general the $A_{lk}$ is comprised of cortically local, cortically distant and extracortical/subcortical axonal pulses. Because subcortical and cortically distant axonal pulses arise exclusively from excitatory neurons, $A_{ek}$ and $A_{ik}$ are defined as

$$A_{ek}(r,t) = N_{ek}^{\beta} S_e\left[h_e(r,t)\right] + \phi_{ek}(r,t) + p_{ek}(r,t)\ , \tag{14.3}$$

$$A_{ik}(r,t) = N_{ik}^{\beta} S_i\left[h_i(r,t)\right]\ , \tag{14.4}$$

where $N_{lk}^{\beta} S_l$, the mean number of connections from local neuronal population $l$ times their mean firing rate $S_l$, models local inputs to target population $k$, $p_{ek}$ represents extracortical (thalamic) excitatory sources and $\phi_{ek}$ pulses arriving across larger distances via the excitatory cortico-cortical fibre system.

The lynchpin of the mean field formulation is the closure of the macroscopic equations (14.1)–(14.4) by the definition of $S_l$. In rate based models it is typically assumed that mean population firing rates are an instantaneous function of the respective mean soma membrane potential. One very general form for $S_l$ in which mean firing rates monotonically increase with $h_k$, are bounded below by zero and above by a maximal firing rate and has a flexible shape is [41]

$$S_l[h_l(r,t)] = S_l^{\max} - S_l^{\max}(1 + \exp\{\sqrt{2}[h_l(r,t) - \mu_l]/\sigma_l\})^{-\kappa_l} \tag{14.5}$$

which for $\kappa_l = 1$ reduces to the well-known symmetric sigmoid function.

Axonal pulses that propagate locally through intracortical fibre systems are assumed to result in conduction delays that are negligible in comparison to the

delays induced by neurotransmitter activation and the passive electrical properties of dendrites. However such delays cannot be ignored for axonal pulses that are propagated by the long range cortico-cortical fibre systems. In the simplest case of a single cortico-cortical conduction velocity $v_{ek}$ and an exponential fall off in the strength of cortico-cortical connectivity with increasing distance between source and target neuronal populations of characteristic scale $1/\Lambda_{ek}$ it can be shown that the propagation of $\phi_{ek}$ can be approximately described by the following two-dimensional telegraph equation

$$\left[(\partial_t + v_{ek}\Lambda_{ek})^2 - \frac{3}{2}v_{ek}^2\nabla^2\right]\phi_{ek}(r,t) = v_{ek}^2\,\Lambda_{ek}^2\,N_{ek}^{\alpha}\,S_e\left[h_e(r,t)\right] , \qquad (14.6)$$

where $N_{ek}^{\alpha}$ is the total number of excitatory synaptic connections formed by long-range cortico-cortical axons on local population $k$. Robinson et al. [65] and Jirsa and Haken [37] have both defined similar long-range propagators.

Equations (14.1)–(14.6) typically define the model of Liley et al. and in addition to being able to reproduce the main features of spontaneous human EEG gives rise to a rich repertoire of interesting and/or novel dynamical activity.

### *14.2.1 Model Extensions*

While the physiological specificity of the model of Liley can be easily extended by the addition of sub-populations of excitatory and inhibitory neurons or by the inclusion of ancillary axonal conduction systems of differing characteristic scales and conduction velocities, the resulting formulation, while arguably of greater biological veracity, will have a substantially augmented phase space. In non-linear systems larger phase spaces make it more difficult to characterise system dynamics. It is therefore fortunate that there are a number of modifications and extensions that can be made to the model of Liley et al. that further supplement its physiological relevance without causing its phase space to expand. Further such modifications can be utilised by other mean field approaches aimed at modelling cortical electrorhythmogenesis.

A simple modification of the equation describing the dynamics of the postsynaptic currents enables independent adjustments of the rise and decay times of the unitary postsynaptic potential so defined [11]. By defining $I_{lk}$ to satisfy

$$[\partial_t + \gamma(\epsilon)][\partial_t + \tilde{\gamma}(\epsilon)]I(r,t) = \tilde{\gamma}(\epsilon)e^{\gamma(\epsilon)/\gamma_0}\Gamma\cdot A(r,t) , \qquad (14.7)$$

$$\gamma(\epsilon) = \epsilon\gamma_0/(e^{\epsilon}-1) , \tilde{\gamma} = \gamma(\epsilon)e^{\epsilon} \qquad (14.8)$$

where we have dropped the subscripts for clarity, $1/\gamma_0$ defines the time to peak of, and $\epsilon > 0$ controls the decay of, the unitary postsynaptic potential. It is worth noting that Eq. (14.7) reduces to Eq. (14.2) as $\epsilon \to 0$.

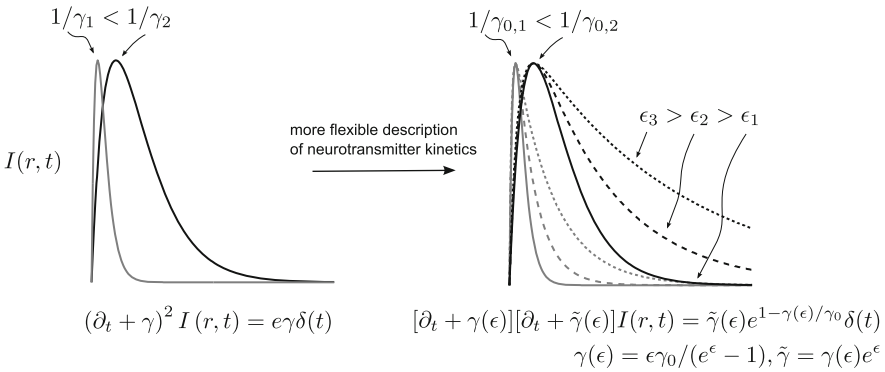


**Fig. 14.2** The independent adjustment of the rise and decay times of the modelled unitary postsynaptic potential enables the more faithful modelling of physiologically and pharmacologically induced alterations in bulk neurotransmitter kinetics and dendritic cable properties

Why might such a formulation be useful? Firstly, isoflurane, a volatile halogenated anaesthetic, has been shown to prolong the decay time of the unitary inhibitory postsynaptic potential as well as reducing the peak amplitude of both excitatory and inhibitory postsynaptic potentials [7, 49]. Based on experiment $\gamma_0$, $\epsilon$ and $\Gamma$ can then be defined to be functions of extracellular anaesthetic concentration such that the effects of isoflurane on the EEG can be modelled. By taking this approach Bojak and Liley [11] have been able to account for the increases in low frequency power in the human EEG induced by isoflurane action. Secondly, the bulk voltage-dependence of excitatory postsynaptic potential amplitude and time course, that arises as a consequence of a N-methyl-d-aspartate (NMDA)-mediated synaptic component, can plausibly be approximated by such a formulation by allowing $\Gamma$, $\gamma_0$ and $\epsilon$ to be functions of the mean soma membrane potential $h$ i.e. $\Gamma(h)$, $\gamma_0(h)$ and $\epsilon(h)$. At present no work has been performed in this regard however it may offer a fruitful way forward towards modelling the bulk effects of behaviourally or pharmacologically induced alterations in NMDA-mediated receptor activity (Fig. 14.2).

In the model of Liley et al., and other related mean field formulations [37, 56, 65, 72], it is typically assumed that activity propagated between distant cortical areas by the cortico-cortical conduction system is by fibres of relatively uniform conduction velocity. However empirical measurement, either by direct physiological measurement of conduction latencies or indirectly via histological measurement of axonal diameter and the subsequent mapping to conduction velocity, suggests that propagation velocities of the cortico-cortical fibres are instead rather broadly distributed [60, 64]. While such broad distributions are easily incorporated in integral mean field formulations, at least until recently, it has not been possible to include them in the computationally more efficient and tractable mean field partial differential formulations. However as shown in Bojak and Liley [11] by defining $\phi_{ek}$ to satisfy

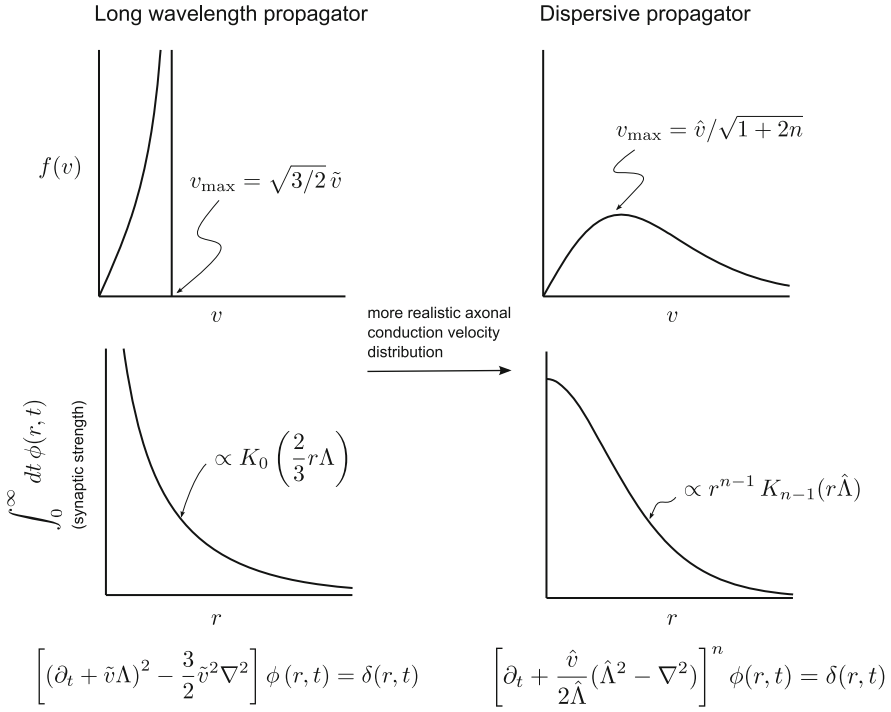


**Fig. 14.3** It is computationally convenient to describe pulse propagation by the long range cortico-cortical conduction system by a partial differential formulation. The long range propagator defined by Eq. (14.6) is simple to implement but assumes that the axonal velocity distribution is sharply peaked (*top left*) about a central value with the synaptic connectivity having an integrable infinite divergence at $r = 0$ (*bottom left*). Empirically however, cortico-cortical axonal velocities are found to be quite broadly distributed. Fortunately a partial differential propagator can be found that assumes a broad distribution of axonal conduction velocities (*top right*) while retaining a monotonic decay in axonal fibre density as a function of distance (*bottom right*)

$$\left[\partial_t + \frac{\hat{v}_{ek}}{2\hat{\Lambda}_{ek}}(\hat{\Lambda}_{ek}^2 - \nabla^2)\right]^n \phi_{ek}(r,t) = 2^{-n}\,\hat{v}_{ek}^n\,\hat{\Lambda}_{ek}^n\,N_{ek}^{\alpha}\,S_e[h(r,t)] \tag{14.9}$$

a marginal velocity distribution, $f_{ek}(v)$, of the form

$$f_{ek}(v) = \frac{2nv\hat{v}_{ek}^{2n}}{(v^2 + \hat{v}_{ek}^2)^{n+1}} \tag{14.10}$$

is implied for the propagation of axonal pulses by long-range fibres. Based on fits to callosal fibre data obtained from humans it is estimated that $n = 4$ and $\hat{v}_{ek} \approx 19\,\mathrm{m\,s^{-1}}$. Such a formulation preserves monotonically decreasing connectivity between source and target regions as a function of increasing separation (Fig. 14.3).

## 14.3 Dynamical Features

Despite the structural simplicity of the defining mean field equations, they reveal a rich repertoire of dynamics in the physiologically admissible parameter space. While much of this is of physiological relevance we will in this section restrict our discussion to the dynamical properties and features that have some degree of mathematical novelty.

### *14.3.1 A Novel Route to Chaos*

The brain is undoubtably a structured and highly complex dynamical system. Attempts to characterise and explain the structured emergence of such complex activity face many hurdles not the least of which is experimental. How do we measure the state of a complex system in the presence of substantial physiological measurement noise? Attempts to determine whether the brain supports the existence of deterministic dynamical macroscopic brain states are inevitably frustrated by the noisy and non-stationary time series data obtained from EEG, MEG or resting state fMRI. Might the existence of theoretical evidence for such complexity help guide and motivate such empirical explorations? In this regard the chaotic dynamical behaviour of a macrocolumnar reduction of the Liley model, and its parametric organization, might be relevant to this quest. By ignoring long range connectivity the Liley model's phase space can be dramatically reduced in size – yet retain considerable dynamical complexity. For example by assuming $\gamma_{ik} \equiv \gamma_i$, $\gamma_{ek} \equiv \gamma_e$ $N^{\alpha}_{ek} = 0$, and under some weak assumptions of convergence, Eqs. (14.1)–(14.4) can be rewritten as [15]

$$\tau_k \partial_t h_k = h^r_k - h_k + \sum_{l=e,i} e\Gamma_{lk} \frac{h^{eq}_{lk} - h_k}{|h^{eq}_{lk} - h^r_k|} \{\gamma_l N^{\beta}_{lk} I_l + (1 - \delta_{lk})[p_{lk} - N^{\beta}_{lk} p_l]/\gamma_l\} \tag{14.11}$$

$$(\partial_t + \gamma_k)^2 I_k = S_k(h_k) + p_k \tag{14.12}$$

where $p_e = p_{ee}/N^{\beta}_{ee}$, $p_i = p_{ii}/N^{\beta}_{ii}$ and $\delta_{lk}$ is the Kronecker delta. It is worth noting that our "synaptic currents" have been trivially rescaled to have units of $s^{-1}$. For a range of physiologically admissible parameter values these simplified equations are, not surprisingly, capable of producing aperiodic behaviour characteristic of deterministic chaos. However what is perhaps surprising is that such chaotic activity arises through a number of routes, one of which is quite unusual. Initial numerical explorations involving the full set of equations, in which long range connectivity was ignored, revealed extensive chaos in a parameter plane defined by $p_{ee}$ and $p_{ei}$. Subsequently it was shown that such chaos was spawned by a co-dimension one homoclinic bifurcation, known as a Shil'nikov saddle-node

bifurcation[3] located in an unphysiological region of the $(p_{ee}, p_{ei})$ parameter plane [75]. However, even though this co-dimension one bifurcation is located in an unphysiological region of parameter space it nevertheless organizes the qualitative behaviour of the emerging dynamics in the physiological meaningful parameter space. Interestingly this route to chaos occurs in the vicinity of a codimension three, focus type, degenerate Bogdanov-Takens point, suggesting that there might exist an *organising centre* for the qualitative organization of dynamics in an even larger region of parameter space. Importantly for *the same* parameter set the reduced Eqs. (14.11) also give rise to chaos [15] in the $(p_{ee}, p_{ei})$ parameter plane spawned by an identical Shil'nikov saddle-node bifurcation at unphysiological (i.e. negative) values of $p_{ee}$ and $p_{ei}$. Such a reduction may therefore aid in the efficient characterisation of high co-dimension organising centres.

### *14.3.2 Metabifurcations*

One of the limitations in performing a bifurcation analysis on a high dimensional system is the difficulty in establishing a canonical parameter set from which to explore the qualitative organization of the parameter space and to relate it to physiologically meaningful or significant behaviour. Often parameter sets are degenerate, in the sense that parametrically widely separated sets can produce similar, physiologically relevant, behaviour. For example [25] numerically generated over 70,000 parameter sets for the spatially homogeneous (i.e. $\nabla^2\phi_{ek} = 0$) Liley model that gave rise to electroencephalographically and physiologically plausible behaviour: parameters within empirically established ranges, alpha band oscillatory activity, '$1/f$' low frequency activity and modelled mean neuronal firing rates $\lesssim 20\,\mathrm{s}^{-1}$. A subsequent principal components analysis revealed that the first ten principal components cumulatively accounted for less than 50 % of the total parametric variance i.e. the structure of the parameter space could not be appreciably simplified by assuming linear combinations of parameters. Therefore how might we investigate the qualitative dynamical properties of the model's physiological admissible parameter space? One possible solution is to attempt to partition the parameter space based on a classification of the patterns of bifurcation diagrams obtained by continuing in one or more appropriately chosen parameters, and to determine the conditions under which, if any, inter-bifurcation pattern transition occurs. We refer to such a general method as a "*metabifurcation analysis*".

[3]If a saddle node has a single homoclinic orbit, then a unique limit cycle will form when the equilibrium disappears. This is often referred to as a saddle-node on an invariant circle bifurcation. If a saddle node has two or more homoclinic orbits then infinitely many saddle limit cycles (i.e. chaos) appear when the equilibrium disappears. In general this is referred to as a Shil'nikov saddle-node bifurcation. These bifurcations should not be confused with either saddle node (fold) or saddle-homoclinic bifurcations.

How might such a metabifurcation analysis proceed? It is known that in the Liley model inhibition is found to be a very sensitive locus of dynamical control. Small alterations in modelled inhibitory coupling strengths and neurotransmitter kinetics sensitively induce changes in model stability, excitability and frequencies of driven and autonomous oscillatory modes. It has been theorised that such sensitivity can explain many of the electroencephalographic features of $\gamma$-amino butyric acid (GABA)-ergic anaesthetic action (see Sect. 14.4.1.1). On this basis [25] constructed two-dimensional parameter continuations in an $(R, k)$ plane defined by $\Gamma_{ik} \to R\Gamma_{ik}$ and $N_{ii}^{\beta} \to kN_{ii}^{\beta}$. As $p_{ik} \equiv 0$ variations in $R$ and $k$ enable the independent specification of global and individual population changes in inhibitory input coupling strength. Two dimensional continuations in $(R, k)$ were then performed for a large number of randomly chosen parameter sets, for the spatially homogeneous Liley model, selected to exhibit electroencephalographically and physiological plausible dynamical behaviour.

Based on the analysis of 405 randomly chosen parameter sets it was found that topologically the bifurcation diagrams conformed to two broad patterns or families (Fig. 14.4). For one of the families (F1) two, almost parallel, lines of saddle-nodes (equilibrium) partition the $(R, k)$ plane into three major regions. For the other family (F2) the $(R, k)$ plane is characterised by the presence of two cusp points, such that the region containing three equilibria is the union of two separated wedge-shaped areas with the cusps as their vertices. In both families emergent Hopf bifurcations interact with the saddle node bifurcations by so-called fold-Hopf points. The two families could be distinguished by differences in the distribution of certain parameters, with the parameter distributions accounting for the greatest dissimilarity being in $\tau_e$, the mean excitatory neuronal membrane time constant, and $\sigma_e$, the standard deviation in the excitatory neuron mean firing threshold. In particular $\tau_e^{F1}$, $\sigma_e^{F1} < \tau_e^{F2}$, $\sigma_e^{F2}$. In general it is found that parameter sets belonging to F1 are associated with a more restricted dynamical repertoire than parameter sets belonging to F2.

Topological transitions between the two types of families can be induced by changes in $p_{ee}$ and $p_{ei}$. In general reductions in $p_{ei}$ in parameter sets belonging to F1 result in the topological metamorphosis of the $(R, k)$ bifurcation diagram to that of F2. Specifically decreasing $p_{ei}$ results in the appearance of two cusp points via a so-called *swallow tail* bifurcation until the bifurcation diagram resembles that of F2. A similar topological transition is induced from F1 to F2 if a metabifurcation parameter $p_{ee}$ is instead increased.

What, if at all, might be the physiological significance of such "*metabifurcations*"? Two speculations present themselves. Firstly the metabifurcation parameters $p_{ee}$ and $p_{ei}$ model thalamic input, and therefore suggest an alternative role for thalamus other than its classically defined character as a relay station for peripherally derived sensory information. Because changes in $p_{ee}$ and $p_{ei}$ transfigure the topological organization of bifurcations in the $(R, k)$ plane we might hypothesise that thalamic activity modulates, and in a sense selects, the cortical dynamical landscape. Viewed from this perspective sensory input may be conceived as configuring the possible domain of the cortical response in addition to initiating it. Further by

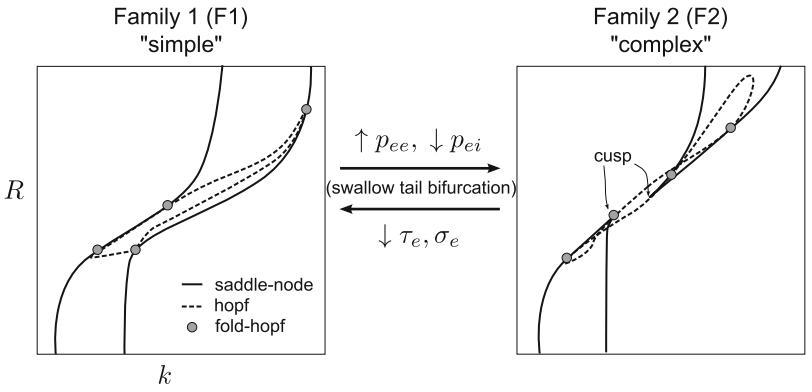


**Fig. 14.4** Schematic diagram illustrating two topological families of bifurcation diagrams obtained by the classification of continuations in the $(R, k)$ parameter plane of ≈400 parameter sets chosen to exhibit physiologically and electroencephalographically admissible behaviour. Also illustrated are the parameters identified to most sensitively effect topological transitions between the two families. Numerical analysis reveals that parameter sets belonging to family 1 have a more restricted repertoire of dynamical behaviour than those belonging to family 2. For further details see [25] (Figure adapted from [25])

considering thalamocortical feedback the possibility is opened up for some form of auto-regulation of cortical dynamics: cortical feedback through thalamus could initiate a sequence of transitions between topologically distinct bifurcation patterns and thus the cortical dynamical repertoire could be reconfigured "*on the fly*", and on a time scale quite distinct to activity dependent synaptic plasticity. The second speculation concerns activity dependent changes in $\tau_e$ and $\sigma_e$. The widely held view is that learning principally involves modifications of synaptic strength. However there exists an alternative, though less well known, view in which learning may also involve non-synaptic processes, such as modulations in voltage dependent membrane conductances, that manifest themselves in alterations in neuronal excitability [52]. For example widely identified non-synaptic changes observed during learning include changes in neuronal input resistance and alterations in neuronal burst/spike threshold. The mean field correlates of these single neuron properties include $\tau_e$ and $\sigma_e$. Thus we might speculate that activity dependent changes in $\tau_e$ and $\sigma_e$ cause long lasting changes in the cortical dynamical landscape, and that these alterations contribute to the behavioural changes observed during learning.

### *14.3.3 Multistability*

Many systems in nature exhibit multistability: when starting from different initial conditions the system can evolve into different attractors with quite different long term behaviour. The term "*generalised multistability*" was coined in order to

distinguish it from "*trivial multistability*" which arises from the co-existence of multiple stable fixed points. Subsequent to its initial theoretical and experimental delineation it is now a well described phenomenon in neuroscience, optics and condensed matter physics.

In neuroscience one of the most extensive examples of generalised multistability is found in the R15 *Aplysia* neuron model in which five different limit cycles and two chaotic attractors are found to co-exist [16]. Functionally multistability might provide a mechanism whereby transient changes in neural activity or sensory input induce persistent changes in oscillatory activity. Such oscillatory mode shifts may therefore directly initiate changes in behaviour or perception, or act as a dynamical substrate from which further activity dependent modulations in dynamics arise. While relatively well studied in the context of single neuron dynamics, multistability at the cortical population level has been little appraised either experimentally or theoretically. However emerging evidence does suggest that resting alpha (8–13 Hz) band activity can be decomposed into distinct high and low amplitude modes [27], and that this can be interpreted as evidence for cortical population level multistability [28]. It is therefore natural to ask whether such multistable activity can be found in the Liley model.

It is shown in [20] that a macrocolumnar version (i.e. $N_{ek}^{\alpha} = 0$) of the Liley model is able to support the co-existence of two limit cycle attractors and one chaotic attractor in an initial condition space. The limit cycle attractors consist of (i) a high amplitude, high firing rate ($\approx 300\,\mathrm{s}^{-1}$), limit cycle with a dominant frequency of $\approx 5$ Hz and a strong first harmonic $\approx 10$ Hz, and (ii) a low amplitude, low firing rate ($\approx 20\,\mathrm{s}^{-1}$), limit cycle with a dominant frequency of $\approx 10$ Hz. The set of initial conditions which gives rise to the low amplitude limit cycle is embedded in a sea of initial conditions which gives rise to a small amplitude chaotic attractor (largest Lyapunov exponent $= 3.4\,\mathrm{s}^{-1}$; Kaplan-Yorke dimension $= 2.086 \pm 0.003$) having a dominant frequency in the alpha band. Surrounding the initial conditions of these low amplitude dynamics is an extensive region of large-amplitude limit cycle dynamics.

Unlike multistable dynamics observed in a similar mean field model [28], the multistable dynamics in this model does not arise due to noise driving in the vicinity of a sub-critical Hopf bifurcation. Parametric continuations in $p_{ee}$ instead reveals that a high amplitude limit cycle, born from a subcritical Hopf bifurcation at large $p_{ee}$, surrounds chaos born through a period doubling cascade at small $p_{ee}$ in which is embedded a low amplitude limit cycle orbit that appears to arise through a homoclinic bifurcation at intermediate values of $p_{ee}$.

## 14.4 Physiological Relevance

One of the strengths of the model of Liley is the physiological relevance of its parameterisation. All model parameters correspond to quantities that can be physiologically and anatomically independently measured, and thus the important

question can be asked: to what extent does the physiologically admissible model parameter space produce behaviour that is both physiologically and electroencephalographically tenable? For example can the model of Liley account for the electroencephalographically observed alpha rhythm in the context of a physiologically meaningful parameterisation? Being able to account for the alpha rhythm would signal the suitability of this model as one basis to account for bulk perturbations in dynamical brain activity that are observed to occur in health, disease and during drug administration.

### *14.4.1 The Resting Alpha Rhythm*

Between 1926 and 1929 Hans Berger laid the foundations for the development of electroencephalography in humans [32]. While canine EEG had been discovered many decades earlier [17], it was Berger who first described the alpha rhythm (8–13 Hz), its occipital dominance and its attenuation in response to mental effort and opening of the eyes. The intervening years have revealed that alpha band activity is not restricted to occipital cortex. Alpha band activity is recordable over much of the cortical surface and is reactive (i.e. enhanced or attenuated) in response to a much wider variety of cognitive activity than just opening and closing the eyes. For this reason it is often preferable to refer to 8–13 Hz electroencephalographic activity as *alpha band activity* rather than as the *alpha rhythm*.

Despite amassing a great deal of knowledge regarding the phenomenology of alpha band activity we remain comparatively ignorant regarding the physiological basis for its genesis: does it (i) arise from intrinsic oscillatory activity in individual cortical neurons (ii) stem from oscillatory thalamic activity directly driving populations of cortical neurons or (iii) emerge through the reverberant activity generated by reciprocal interactions of synaptically connected neuronal populations in cortex, and/or through such reciprocal interactions between cortex and thalamus? Theoretically the last of these is the most interesting and the one best addressed by the mean field modelling approach. Specifically, for a range of physiologically admissible parameter values the model of Liley reveals a wide array of deterministic and noise-driven dynamics that includes alpha band activity [11, 41]. In particular, physiologically plausible alpha band activity can appear in three distinct dynamical scenarios: linear noise driven, limit-cycle, and chaotic dynamics. For appropriate parameterisations linearisations of the defining equations about a stable singular point reveals alpha band oscillatory activity in $h_e$ and $h_i$ at physiologically plausible firing rates (0.1–20 $s^{-1}$), as well as rhythmic activity in other bands of electroencephalographic interest. In the case of electroencephalographically plausible alpha band activity (full-width-half-maximum of the peak alpha band frequency $\gtrsim 5$) linearisation reveals model activity to be essentially determined by conjugate pairs of weakly damped poles at alpha band frequencies. The physiological plausibility of these linearisations suggests that resting EEG may be viewed as a filtered random linear process. Indeed empirical analysis has found that, except for short bursts

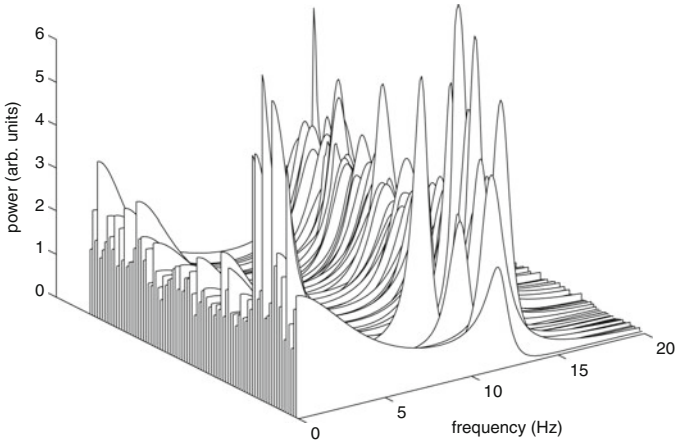


**Fig. 14.5** Analytical fluctuation spectra for 86 physiologically admissible parameter sets chosen to exhibit plausible mean resting neuronal firing rates and resting alpha band activity, as well as a biphasic surge during simulated anaesthetic action. For details of parameters and method of calculation refer to [11]

of subdural and scalp-recorded EEG, the alpha rhythm is indistinguishable from linearly filtered white noise [70, 71]. On this basis we might reasonably assert that "resting" cortex is dynamically in a state of marginal linear stability.

In the Liley model, based on a range of heuristic search strategies [11], physiologically and electroencephalographically plausible alpha band activity is found to be widely, but sparsely, distributed over the whole biologically valid parameter space without easily discernable structure in most parameter dimensions. For example by randomly searching the physiologically admissible parameter space [11] found that of $7 \times 10^9$ randomly generated parameter sets 73,454 ($\approx$0.001 %) produced electroencephalographically plausible alpha band activity (Fig. 14.5). However as it is likely there are biological co-dependencies between various model parameters such sparseness may be artificial.

By analysing the response of model dynamics to small parameter perturbations it is found that emergent alpha band activity is particularly sensitive to alterations in those parameters that characterise inhibitory action. This in turn suggests a novel mechanism for alpha band rhythmogenesis: alpha band oscillatory activity arises from reverberant activity between populations of inhibitory interneurons. To see this consider the following sequence of events – (i) initially (basally) excited inhibitory neurons, following a delay related to the characteristic time of inhibitory neurotransmitter kinetics, are inhibited due to negative feedback and thus inhibitory neuronal firing rates decrease (ii) because the activity of inhibitory neurons has decreased feedback inhibition is reduced and thus inhibitory neuronal firing rates increase again and return to basal levels on a time scale related to the characteristic time of inhibitory neurotransmitter kinetics (iii) once mean inhibitory firing rates return to basal levels feedback inhibition between inhibitory

neurons is again strengthened and mean inhibitory firing rate again decrease and the cycle then repeats. Such oscillatory activity then "slaves" population excitatory neuronal activity and thus gives rise to alpha band variations in scalp recorded electroencephalographic activity [43].

Thus the model of Liley hypothesises that (i) resting alpha band activity is a marginally stable rhythm and (ii) inhibition is a sensitive locus for the dynamical control of alpha band oscillations. These hypotheses have important implications for the functional role of alpha band oscillations during cognition and their physiological control and pharmacological modulation. For example parameter sets chosen to produce electroencephalographically plausible linear noise driven alpha, as well as a surge in total EEG power during modelled anaesthetic induction, can under small parametric perturbations produce autonomous gamma band (>30 Hz) oscillatory activity. Gamma band oscillations are thought to be the *sine qua non* of cognitive functioning. Indeed there exists much evidence to suggest that the emergence of synchronised gamma-band activity (local field potential or EEG) functional underpins perceptual binding and subserves the processes of cortical computation [29]. Thus the existence of weakly damped, noise-driven, linear alpha activity may be a dynamical precursor to gamma band electroencephalographic activity, and more generally as a physiologically meaningful state from which transitions can be made from or to. From this perspective the alpha rhythms may be better viewed as readiness rhythms and not idling or resting rhythms as is often asserted.

What physiological factors may drive such transitions? Given that cortical population dynamics are hypothesised to be particularly sensitive to variations in inhibitory activity it may represent a target for control by the relatively sparse thalamocortical afferents. Averaged over cortex, less than 2–3 % of all synapses can be attributed to thalamocortical projections [13]. While thalamocortical afferents synapse onto both excitatory (pyramidal) and inhibitory layer IV cortical neurons the strength of such synaptic connections may be far from uniform across the respective target neuronal populations. For example studies in rat barrel cortex show that cortical inhibitory neurons receive thalamocortical synapses that are on average five-fold stronger (in terms of evoked inhibitory postsynaptic amplitude) than those received by nearby pyramidal neurons [50]. In this way relatively weak excitatory thalamocortical input to inhibitory cortical neuronal populations ($p_{ei}$) may be able to precipitate transitions in cortical state. Thus thalamic input arising from either first-order thalamic relay neurons being driven directly by incoming sensory/subcortical input, or from higher-order thalamic relay neurons driven by feedback from cortex, may, rather than only "*driving*" cortex act also to "*modulate*" cortical activity (in the sense of [68]).

While we have speculated that cortical inhibition may be a sensitive target for the control of alpha band activity by thalamocortical afferents at present the empirical evidence for such an assertion is weak. Fortunately stronger evidence for the hypothesised role of inhibitory modulation in the regulation and control of alpha band activity exists. Of particular interest and relevance is the fact that the

endogenous and exogenous pharmacological modulation of GABAergic activity is known to perturb the resting alpha rhythm.

#### 14.4.1.1 Endogenous Pharmacological Modulation

Surprisingly the EEG is known to undergo systematic changes in women during their menstrual cycle. In particular it has been observed that during the late and mid-luteal phases alpha band activity is enhanced. For example [19] observed that the mean occipital alpha band activity increased by 0.3 Hz during the luteal phase and that the average time course of acceleration followed the time course of increases in blood progesterone levels. Similar changes in alpha band activity during oestrus are observed in other studies [6, 9, 61]. How do such changes implicate modulations in GABAergic activity?

Progesterone, a steroid hormone involved in the female menstrual cycle, is metabolised to a high degree to the neurosteroids allopregnanolone and pregnanolone which are potent positive allosteric modulators of GABA subtype A ($GABA_A$) receptor activity such that GABA action is potentiated [33, 62]. These neurosteroids bind to discrete sites on the $GABA_A$ receptors that are distinct to those that bind ethanol, benzodiazepine, barbiturates and a range of general anaesthetic agents. During the mid and late luteal phases progesterone concentrations are highest and thus their effect in modulating GABAergic function is maximal. The model of Liley predicts that the antagonism of GABAergic activity (increases in $\Gamma_{ik}$) should alter the spectral features of resting alpha band activity. In particular the model predicts that increases in $\Gamma_{ii}$ will increase the frequency, and reduce the damping (i.e. reduce the full-width-half-maximum) of the alpha-band linear resonance, whereas increasing $\Gamma_{ie}$ will produce the opposite effect. On this basis the model of Liley would predict that the neurosteroids allopregnanolone and pregnanolone potentiate GABAergic activity in cortical inhibitory neurons to a greater degree than in cortical excitatory neurons. Is such a prediction supported by pharmacological differences in the properties of $GABA_A$ receptors in excitatory and inhibitory neurons?

Structurally $GABA_A$ receptors are composed of 5 membrane spanning protein subunits that are assembled from a family of at least 18 subunits ($\alpha_{1-6}$, $\beta_{1-3}$, $\gamma_{1-3}$, $\sigma_{1-3}$, $\delta$, $\epsilon$, $\theta$) that determine, among other properties, their pharmacological profiles [59]. A range of studies have established that they are heterogeneously distributed across brain areas and neuronal subtypes [30, 58]. In cortex the most abundant receptor isoforms are $\alpha_1\beta_{2/3}\gamma_2$ and $\alpha_2\beta_{2/3}\gamma_2$ differentially localised to inhibitory and excitatory cortical neurons respectively. In general the $\alpha_1\beta_{2/3}\gamma_2$ and $\alpha_2\beta_{2/3}\gamma_2$ isoforms exhibit differential binding affinities for benzodiazepines. Indeed the presence of the $\alpha$ subunit isoform exerts a major effect on the affinity and efficacy of ligands at the benzodiazepine binding site. It is thought that the neurosteroids allopregnanolone and pregnanolone evince similar differential binding affinities based on the demonstrated importance of the $\alpha$ subunit for the binding of neurosteroids [33]. Thus the prediction of the Liley model regarding the

predominant target of neurosteroid action is consistent with the known molecular pharmacology. As the next section will discuss, the differential ligand-binding affinity of GABA receptor isoforms may be relevant to understanding the actions that anesthetics and sedatives have on the EEG.

#### 14.4.1.2 Exogenous Pharmacological Modulation

General anaesthetic agents induce profound reversible alterations in brain activity and behaviour. While positron emission tomography and fMRI have revealed a range of non-uniform reductions in inferred cerebral neuronal activity during anaesthetic drug action [2, 3, 39], to date only changes in the EEG have been reliably correlated with the clinically documented effects of anaesthesia [14]. In general during the progression to deep anaesthesia the EEG undergoes a series of well described quantitative changes: (i) the EEG is transiently activated such that beta band (13–30 Hz) oscillatory activity is increased and alpha band activity is decreased (the so-called "*beta buzz*") (ii) the EEG is slowed (reduction in median and spectral edge frequencies), the alpha rhythm is abolished, and total EEG power transiently increases (the "*biphasic response*") (iii) the appearance of isoelectric (defined as $<5\,\mu$V peak-peak amplitude) periods lasting many seconds separated by short bursts of high amplitude slow, sharp or spiking activity – a phenomenon known as *burst suppression*. While not all anaesthetic agents produce these changes (notable exceptions being nitrous oxide, xenon and ketamine – agents often collectively referred to as "*dissociatives*") they are sufficiently general to motivate systematic processed EEG approaches to the clinical monitoring of depth of anaesthesia.

To what extent can these features be explained by known anaesthetic molecular pharmacology? Countless studies have revealed the synaptic $GABA_A$ receptor to be one of the most important molecular targets mediating the action of anaesthetic and sedative agents [24, 67]. It has been established that a variety of anaesthetic agents reduce the peak amplitude, and selectively prolong the decay, of the inhibitory postsynaptic potential [7]. On this basis [11] have shown that many of the electroencephalographic features of "*typical*" anaesthesia can be accounted for by the model of Liley by utilising a description that enables the independent adjustment of rise and decay times of the inhibitory postsynaptic potential i.e. Eq. (14.7). By parameterising $\Gamma_{ik}$ and $\epsilon_{ik}$ as a function of anaesthetic concentration ($c$) on the basis of experimental measurement, modelled EEG slows, and exhibits a transient increase in total power, with increasing $c$ for appropriately chosen "*base*" parameter sets. While such bulk effects of anaesthetic action can be produced by homogeneous variations of $\Gamma_{ik}$ and $\epsilon_{ik}$, other well known electroencephalographic effects might only be explained by assuming that inhibitory postsynaptic potentials in inhibitory neurons are differentially modulated by anaesthetic action compared to inhibitory postsynaptic potentials in excitatory neurons.

In [43] it was theorised, on the basis of empirical EEG evidence involving the benzodiazepine alprazolam, that the well documented benzodiazepine "*beta*

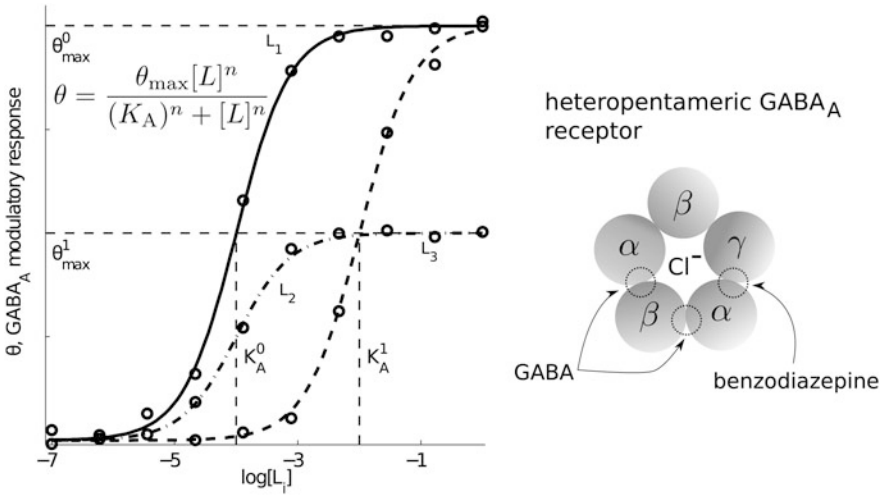


| isoform | abundance | cellular location | sub-cellular location | role |
|---|---|---|---|---|
| $\alpha_1\beta_1\alpha_2$ | 60% | inhibitory | syn./extra syn. | sedation |
| $\alpha_2\beta_3\gamma_2$ | 15-20% | excitatory | synaptic | anxiolysis |
| $\alpha_3\beta_n\gamma_2$ | 10-15% | – | – | – |

**Fig. 14.6** *Top left*: differences in binding affinity, $K_A$, and maximal modulatory response, $\theta^{\max}$, for three hypothetical positive allosteric modulators of the $GABA_A$ receptor. *Top right*: the $GABA_A$ receptor is a co-assembly (oligimer) of five protein subunits, the interfaces of which contain binding sites for GABA and benzodiazepines. *Bottom*: summary of the major $GABA_A$ receptor isoforms found in cortical neurons [30, 51]. The type of $\alpha$ subunits present determines the pharmacological properties of the given isoform. Isoforms containing the $\alpha_1$ subunit have a $BZ_1$-type pharmacology (bind zolpidem and CL218,872 with high affinity), whereas those co-assembled with the $\alpha_2$ isoform have a $BZ_2$-type pharmacology (bind zolpidem and CL218,872 with low affinity)

*buzz*" could be explained by assuming that benzodiazepines acted with greater efficacy at GABAergic synapses on inhibitory neurons that at GABAergic synapses on excitatory neurons (see Fig. 14.6). Such differential potency accords with the empirically established cellular distribution of $GABA_A$ receptor isoforms that exhibit ligand-based differences in the potentiation of GABA induced activity. As discussed previously the high affinity (to zolpidem and CL218,872) $GABA_A$ receptor isoform $\alpha_1\beta_{2/3}\gamma_2$ is found predominantly in cortical inhibitory neurons whereas the low affinity $GABA_A$ receptor isoform $\alpha_2\beta_{2/3}\gamma_2$ is chiefly localised to cortical excitatory neurons [30]. The differential effects of modulating feed-forward and feed-back may also be relevant to understanding the electroencephalographic actions of propofol.

Propofol (2,6-di-isopropylphenol) is a widely used intravenous anaesthetic agent that is distinguished in that, rather than uniformly attenuating alpha band activity, instead elicits strong increases in frontal alpha band (10–13 Hz) activity in addition

to the typical increases in slow wave activity seen with other anaesthetic agents. While it has been suggested that this "alpha" rhythm emerges because propofol enhances feed-forward $GABA_A$ conductances in cortical pyramidal neurons such that thalamocortical feedback is strengthened [18], another possibility suggests itself. Propofol, like the benzodiazepines and the neurosteroids, allosterically enhances GABA-mediated activation of $GABA_A$ receptor activity to a degree depending on its isoform. For example [38] found that in recombinant $GABA_A$ receptors expressed in Xenopus oocytes, that those consisting of the isoform $\alpha_1\beta_{2/3}\gamma_2$ were potentiated to a much greater degree (maximum potentiation compared to baseline $\approx$1,400 %) by propofol than those of the $\alpha_2\beta_{2/3}\gamma_2$ (maximum potentiation compared to baseline $\approx$500 %) isoform. From a theoretical perspective feed-back disinhibition of cortical inhibitory neuronal activity would then be favoured over the feed-forward inhibition of cortical excitatory neuronal activity and thus alpha band activity would be promoted.

### *14.4.2 Mass Action and the Monitoring of Anaesthetic Action*

To date depth of anaesthesia monitoring has relied on a range of heuristic data driven approaches to objectively define optimal levels of hypnosis such that intraoperative awareness is minimised. The most successful of these approaches are arguably those that are based upon the analysis of spontaneous or time locked electroencephalographic activity. Of these approaches the Bispectral Index in particular has become commonplace in clinical anaesthesia [14]. However its use occurs in the context of a number of well documented limitations (i) not all hypnotic agents are reliably detected (e.g. nitrous oxide and the short acting synthetic opioids being quintessential examples), and (ii) the index admits of no clear physiological interpretation as it has been constructed to act as a quantitative surrogate for an ostensibly subjective state.

Given that the model of Liley can offer potential explanation for the electrorhythmogenesis of the resting EEG and its perturbation by a range of factors that include sedative and anaesthetic agents, it may have some utility in monitoring the cerebral effects of general anaesthesia and thus resolve some of the uncertainties associated with the use of the Bispectral Index. While in principle it is possible to estimate parameters of the Liley model on the basis of real data, and to investigate how they correlate with anaesthesia, practically the difficulties are substantial given the model's non-linear partial differential formulation and its high dimensional parameter space. Fortunately many of the model's important qualitative properties can be understood through a linearisation of the form [41,43]

$$H_e(k,\omega) = g(h_e^*,q')\frac{\omega^M + \sum_{m=1}^{M} b_m(k;h_e^*,q)\omega^{M-k}}{\omega^N + \sum_{n=1}^{N} a_n(k;h_e^*,q)\omega^{N-n}} P_{ee}(k,\omega) \tag{14.13}$$

$$= g(h_e^*,q) G_e(k,\omega;h_e^*,q) P_{ee}(k,\omega) \tag{14.14}$$

where it has been assumed that only the excitatory input to the excitatory cortical neuronal population is non-zero. $H_e(k,\omega)$ and $P_{ee}(k,\omega)$ are the Fourier transforms of $h_e(r,t)$ and $p_{ee}(r,t)$ respectively. $G_e(k,\omega;q)$ is defined as the *electrocortical transfer function* and arises from the linearisation about a spatially homogeneous stable singular point $h_e^*$ for a given set of model parameters $q$, and $g(h_e^*,q')$ represents a factored out common term depending on a subset of model parameters $q' \in q$. By assuming $\gamma_{lk} \equiv \gamma_l$ and $\Lambda_{ek} \equiv \Lambda_e$, $N$ and $M$ can be set to 8 and 5 respectively. Such a linearisation reveals that under physiologically plausible parameterisations $G_e(k,\omega)$ gives resonances corresponding to all the major EEG frequency bands [41]. Thus such a linearisation implies that resting EEG can theoretically be understood as arising from a filtered spatio-temporal random process. This is of particular physiological relevance when it is considered that EEG during rest and anaesthesia is typically found to be indistinguishable from a white-noise process [36, 70, 71]. On this basis Eq. (14.13) suggests a quite specific signal processing strategy by which to estimate $G_e(k,\omega)$ and changes in $P_e$. By assuming (i) a matching of poles and zeros in transforming from the continuous to discrete time domains and (ii) a restricted range of wavenumbers $k$ over which physiologically relevant model linear EEG activity occurs Eq. (14.13) can be rewritten in the discrete time domain as [43]

$$H_e(z) = k_d q(q') \frac{1 + \sum_{k=1}^{k=5} b_k(q) z^{-k}}{1 + \sum_{k=1}^{k=8} a_k(q) z^{-k}} P(z) \tag{14.15}$$

where $k_d$ is a constant required to match the gain in going from continuous to discrete time and $z = e^{i\omega/f_s}$ with $f_s$ being the sampling frequency. By assuming $P(z)$ describes a band-limited white-noise process Eq. (14.15) can be written as the following fixed-order autoregressive moving average (ARMA) process

$$h_e[n] = -\sum_{k=1}^{k=8} a_k h_e[n-k] + \sum_{k=0}^{k=5} b_k u[n-k], \text{ or} \tag{14.16}$$

$$A(z) h_e[n] = B(z) u[n] \tag{14.17}$$

where $u[n] \equiv k_d q(q') p[n]$ is a stationary uncorrelated random process and $A(z) = 1 + \sum_{k=1}^{k=8} a_k z^{-k}$ and $B(z) = 1 + \sum_{k=1}^{k=5} b_k z^{-k}$. Tracking the state of this estimated electrocortical filter and its innovating input will provide one possible measure for characterising the cortical effects of anaesthesia. One easily calculated measure of the *state* of the estimated electrocortical filter is the scaled mean pole location, $a_1$. The innovating *input* can be estimated, by assuming that the factor $k_d g(q')$ remains invariant to any intervention, as $\sqrt{\text{Var}[Z^{-1}\{A(z)S(z)/B(z)\}]}$ where $Z^{-1}$ is the inverse $Z$-transform. These respective measures are referred to as the *Cortical State* (CS) and *Cortical Input* respectively, and have been useful in differentiating the electroencephalographic effects of the hypnotic propofol and the analgesic remifentanil (an ultra-short acting synthetic opioid). Figure 14.7 illustrates the

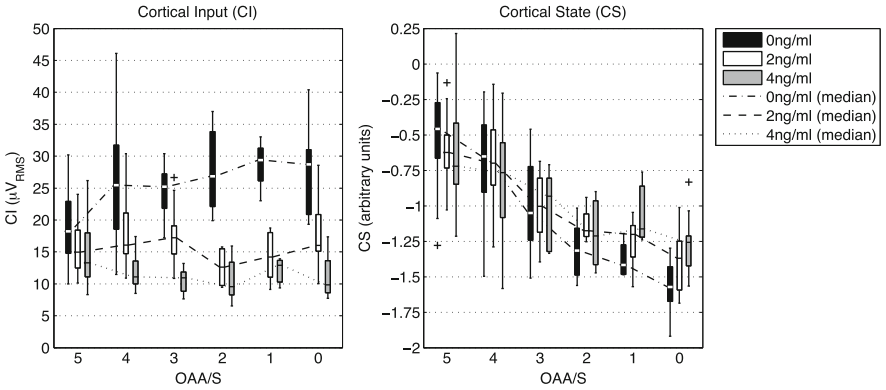


**Fig. 14.7** Box-and-whisker plots for the derived electroencephalographic measures CI and CS, during propofol-remifentanil anaesthesia, as a function of the modified Observer's Assessment of Alertness/Sedation (OAA/S) score for 0, 2 and 4 ng/ml effect site remifentanil concentrations. The modified OAA/S scale is a measure of alertness and sedation: 5 = responds readily to name, 4 = responds lethargically to name, 3 = responds to name called loudly and repeatedly, 2 = responds to mild prodding/shaking, 1 = responds only after painful stimulus, 0 = completely unresponsive. *Boxes* represent interquartile ranges, *lines enclosed within boxes* median values, *whiskers* represent largest/smallest values and crosses outliers (Figure adapted from [44])

differences in the response of CS and CI as a function of the Observers Assessment of Alertness/Sedation (OAA/S) (OAA/S = 5 is fully responsive, OAA/S = 0 is completely unresponsive) and the level of analgesia (0, 2 or 4 ng/ml remifentanil). On this basis we can speculate that CS is a measure of *hypnosis* and CI is a measure of *nociception*.

## 14.5 Conclusion

The aim of this chapter has been to give an account of a relatively simple neural field model of the resting EEG and to briefly illustrate some of its more interesting dynamical features as well as speculating on its physiological relevance in accounting for resting alpha band activity and its perturbation by a range of endogenous and exogenous pharmacological factors. In particular we discussed the predicted sensitivity of model dynamics to differential perturbations in cortical inhibition and how this might account for the electroencephalographic effects of anesthetics that act principally through GABAergic agonism. We argued that to first approximation anesthetics alter noise-driven linear properties of the resting EEG. However it is known that anesthetics are also able to induce quite profound qualitative alterations in the EEG. At high levels of many sedative and anaesthetic agents the EEG can exhibit burst suppression. Typically the burst suppression pattern consists of bursts of high amplitude slow, sharp or spiking activity separated

by periods of near iso-electricity (suppression) [54]. As anaesthetic depth increases the periods of burst become shorter. While it is often assumed that the burst-suppression pattern arises from slow thalamic oscillations driving cortex, the fact that the pattern survives following cortical deafferentation suggests that it arises as a consequence of intrinsic dynamical properties of cortical tissue. Therefore the challenge of ours, and similar models, is to account for this phenomenon in the context of a plausible physiological framework and the known molecular and cellular targets associated with anaesthetic action.

There is an emerging practical utility for mean field models as evinced by our simple fixed order ARMA approach. While this single-electrode approach can, at least in principle, be easily extended to the multi-electrode case by the suitable definition of a multivariate (vector) ARMA model the real challenge is to estimate actual model parameters from empirical data and to see if they accord with known physiology. At present the action of anaesthetic agents would appear to provide the most robust context in which to estimate model parameters as they can be directly associated with known cellular and molecular targets of action.

## References

1. Adrian, E., Matthews, B.: The berger rhythm, potential changes from the occipital lobe in man. Brain **57**, 355–385 (1934)
2. Alkire, M.T.: Probing the mind: anesthesia and neuroimaging. Clin. Pharmacol. Ther. **84**(1), 149–152 (2008)
3. Alkire, M.T., Haier, R.J., Barker, S.J., Shah, N.K., Wu, J.C., Kao, Y.J.: Cerebral metabolism during propofol anesthesia in humans studied with positron emission tomography. Anesthesiology **82**(2), 393–403 (1995)
4. Amari, S.: Homogeneous nets of neuron-like elements. Biol. Cybern. **17**, 211–220 (1975)
5. Andersen, P., Andersson, S.: Physiological Basis of the Alpha Rhythm. Appelton-Century-Crofts, New York (1968)
6. Baker, F.C., Colrain, I.M.: Daytime sleepiness, psychomotor performance, waking EEG spectra and evoked potentials in women with severe premenstrual syndrome. J. Sleep Res. **19**(1 Pt 2), 214–227 (2010)
7. Banks, M.I., Pearce, R.A.: Dual actions of volatile anesthetics on GABA(A) IPSCs: dissociation of blocking and prolonging effects. Anesthesiology **90**(1), 120–134 (1999)
8. Barth, A.L., Poulet, J.F.: Experimental evidence for sparse firing in the neocortex. Trends Neurosci. **35**(6), 345–355 (2012)
9. Becker, D., Creutzfeldt, O.D., Schwibbe, M., Wuttke, W.: Changes in physiological, EEG and psychological parameters in women during the spontaneous menstrual cycle and following oral contraceptives. Psychoneuroendocrinology **7**(1), 75–90 (1982)
10. Beurle, R.: Properties of a mass of cells capable of regenerating pulses. Phil. Trans. R. Soc. B **240**, 55–94 (1956)
11. Bojak, I., Liley, D.: Modeling the effects of anesthesia on the electroencephalogram. Phys. Rev. E **71**, 041902 (2005)
12. Borst, J.G.: The low synaptic release probability in vivo. Trends Neurosci. **33**(6), 259–266 (2010)
13. Braitenberg, V., Schüz, A.: Cortex: Statistics and Geometry of Neuronal Connectivity, 2nd edn. Springer, New York (1998)

14. Bruhn, J., Myles, P.S., Sneyd, R., Struys, M.M.: Depth of anaesthesia monitoring: what's available, what's validated and what's next? Br. J. Anaesth. **97**(1), 85–94 (2006)
15. Buente, D., Frascoli, F., Liley, D.: Complex dynamics for a reduced model of human eeg: implications for the physiological basis of brain activity. BMC Neurosci. **12**, 198 (2011)
16. Canavier, C.C., Baxter, D.A., Clark, J.W., Byrne, J.H.: Nonlinear dynamics in a model neuron provide a novel mechanism for transient synaptic inputs to produce long-term alterations of postsynaptic activity. J. Neurophysiol. **69**(6), 2252–2257 (1993)
17. Caton, R.: The electric currents of the brain. Br. Med. J. **2**, 278 (1875)
18. Ching, S., Cimenser, A., Purdon, P.L., Brown, E.N., Kopell, N.J.: Thalamocortical model for a propofol-induced alpha-rhythm associated with loss of consciousness. Proc. Natl. Acad. Sci. U.S.A. **107**(52), 22665–22670 (2010)
19. Creutzfeldt, O.D., Arnold, P.M., Becker, D., Langenstein, S., Tirsch, W., Wilhelm, H., Wuttke, W.: EEG changes during spontaneous and controlled menstrual cycles and their correlation with psychological performance. Electroencephalogr. Clin. Neurophysiol. **40**(2), 113–131 (1976)
20. Dafilis, M., Frascoli, F., Cadusch, P., Liley, D.: Chaos and generalised multistability in a mesoscopic model of the electroencephalogram. Physica D **13**, 1056–1060 (2009)
21. David, O., Kiebel, S., Harrison, L., Mattout, J., Kilner, J., Friston, K.: Dynamic causal modeling of evoked responses in EEG and MEG. NeuroImage **30**, 1255–1272 (2006)
22. Deco, G., Jirsa, V., Robinson, P., Breakspear, M., Friston, K.: The dynamic brain: from spiking neurons to neural masses and cortical fields. PLoS Comput. Biol. **4**, e1000092 (2008)
23. De-Miguel, F.F., Fuxe, K.: Extrasynaptic neurotransmission as a way of modulating neuronal functions. Front. Physiol. **3**, 16 (2012)
24. Franks, N.P.: General anaesthesia: from molecular targets to neuronal pathways of sleep and arousal. Nat. Rev. Neurosci. **9**, 370–386 (2008)
25. Frascoli, F., van Veen, L., Bojak, I., Liley, D.: Metabifurcation analysis of a mean field model of the cortex. Physica D **240**, 949–62 (2011)
26. Freeman, W.: Mass Action in the Nervous System: Examination of the Neurophysiological Basis of Adaptive Behavior Through the EEG, 1st edn. Academic, New York (1975). Also electronic edn.: http://sulcus.berkeley.edu/MANSWWW/MANSWWW.html (2004)
27. Freyer, F., Aquino, K., Robinson, P.A., Ritter, P., Breakspear, M.: Bistability and non-Gaussian fluctuations in spontaneous cortical activity. J. Neurosci. **29**(26), 8512–8524 (2009)
28. Freyer, F., Roberts, J.A., Becker, R., Robinson, P.A., Ritter, P., Breakspear, M.: Biophysical mechanisms of multistability in resting-state cortical rhythms. J. Neurosci. **31**(17), 6353–6361 (2011)
29. Fries, P.: Neuronal gamma-band synchronization as a fundamental process in cortical computation. Annu. Rev. Neurosci. **32**, 209–224 (2009)
30. Fritschy, J.M., Mohler, H.: GABAA-receptor heterogeneity in the adult rat brain: differential regional and cellular distribution of seven major subunits. J. Comp. Neurol. **359**(1), 154–194 (1995)
31. Giaume, C., Koulakoff, A., Roux, L., Holcman, D., Rouach, N.: Astroglial networks: a step further in neuroglial and gliovascular interactions. Nat. Rev. Neurosci. **11**, 87–99 (2010)
32. Gloor, P.: Hans Berger on the electroencephalogram of man. Electroencephalogr. Clin. Neurophysiol. **S28**, 350 (1969)
33. Hosie, A.M., Clarke, L., da Silva, H., Smart, T.G.: Conserved site for neurosteroid modulation of GABA A receptors. Neuropharmacology **56**(1), 149–154 (2009)
34. Hutt, A. (ed.): Sleep and Anesthesia: Neural Correlates in Theory and Experiment. Springer Series in Computational Neuroscience. Springer, New York (2011)
35. Jansen, B.H., Rit, V.G.: Electroencephalogram and visual evoked potential generation in a mathematical model of coupled cortical columns. Biol. Cybern. **73**(4), 357–366 (1995)
36. Jeleazcov, C., Fechner, J., Schwilden, H.: Electroencephalogram monitoring during anesthesia with propofol and alfentanil: the impact of second order spectral analysis. Anesth. Analg. **100**(5), 1365–1369 (2005)

37. Jirsa, V., Haken, H.: Field theory of electromagnetic brain activity. Phys. Rev. Lett. **77**, 960–963 (1996)
38. Lam, D.W., Reynolds, J.N.: Modulatory and direct effects of propofol on recombinant GABAA receptors expressed in xenopus oocytes: influence of alpha- and gamma2-subunits. Brain Res. **784**(1–2), 179–187 (1998)
39. Langsjo, J.W., Alkire, M.T., Kaskinoro, K., Hayama, H., Maksimow, A., Kaisti, K.K., Aalto, S., Aantaa, R., Jaaskelainen, S.K., Revonsuo, A., Scheinin, H.: Returning from oblivion: imaging the neural core of consciousness. J. Neurosci. **32**(14), 4935–4943 (2012)
40. Liley, D., Cadusch, P., Wright, J.: A continuum theory of electro-cortical activity. Neurocomputing **26–27**, 795–800 (1999)
41. Liley, D., Cadusch, P., Dafilis, M.: A spatially continuous mean field theory of electrocortical activity. Netw.: Comput. Neural Syst. **13**, 67–113 (2002)
42. Liley, D., Cadusch, P., Dafilis, M.: Corrigendum. Netw.: Comput. Neural Syst. **14**, 369 (2003)
43. Liley, D., Cadusch, P., Gray, M., Nathan, P.: Drug-induced modification of the system properties associated with spontaneous human electroencephalographic activity. Phys. Rev. E **68**, 051906 (2003)
44. Liley, D., Sinclair, N., Lipping, T., Heyse, B., Vereecke, E., Struys, M.: Propofol and remifentanil differentially modulate frontal electroencephalographic activity. Anesthesiology **113**, 1–13 (2010)
45. Liley, D., Foster, B., Bojak, I.: A mesoscopic modelling approach to characterising anaesthetic action on brain electrical activity. In: Hutt, A. (ed.) Sleep and Anesthesia: Neural Correlates in Theory and Experiment. Springer Series in Computational Neuroscience, pp. 139–66. Springer, New York (2011)
46. Liley, D., Foster, B., Bojak, I.: Co-operative populations of neurons: mean field models of mesoscopic brain activity. In: Le Novère, N. (ed.) Computational Systems Neurobiology, pp. 317–64. Springer, New York (2012)
47. Llinas, R.: The intrinsic electrophysiological properties of mammalian neurons: insights into central nervous system function. Science **242**, 1654–1664 (1988)
48. Lopes da Silva, F.: Dynamics of EEGs as signals of neuronal populations: models and theoretical considerations. In: Niedermeyer, E., Lopes da Silva, F. (eds.) Electroencephalography: Basic Principles, Clinical Applications, and Related Fields, pp. 85–106, 5th edn. Lippincott Williams & Wilkins, Philadelphia (2005)
49. Maclver, M.B., Mikulec, A.A., Amagasu, S.M., Monroe, F.A.: Volatile anesthetics depress glutamate transmission via presynaptic actions. Anesthesiology **85**(4), 823–834 (1996)
50. Miller, K.D., Pinto, D.J., Simons, D.J.: Processing in layer 4 of the neocortical circuit: new insights from visual and somatosensory cortex. Curr. Opin. Neurobiol. **11**(4), 488–497 (2001)
51. Mohler, H., Fritschy, J.M., Rudolph, U.: A new benzodiazepine pharmacology. J. Pharmacol. Exp. Ther. **300**(1), 2–8 (2002)
52. Mozzachiodi, R., Byrne, J.H.: More than synaptic plasticity: role of nonsynaptic plasticity in learning and memory. Trends Neurosci. **33**(1), 17–26 (2010)
53. Niedermyer, N.: The normal EEG of the waking adult. In: Niedermeyer, E., Lopes da Silva, F. (eds.) Electroencephalography: Basic Principles, Clinical Applications, and Related Fields, pp. 167–192, 5th edn. Lippincott Williams & Wilkins, Philadelphia (2005)
54. Niedermeyer, E.: The burst-suppression electroencephalogram. Am. J. Electroneurodiagnostic Technol. **49**(4), 333–341 (2009)
55. Niedermeyer, E., Lopes da Silva, F. (eds.): Electroencephalography: Basic Principles, Clinical Applications, and Related Fields, 5th edn. Lippincott Williams & Wilkins, Philadelphia (2005)
56. Nunez, P.: The brain wave equation: a model for the EEG. Math. Biosci. **21**, 279–297 (1974)
57. Nunez, P., Srinivasan, R.: Electric Fields of the Brain: The Neurophysics of EEG, 2nd edn. Oxford University Press, New York (2005)
58. Nutt, D.: GABAA receptors: subtypes, regional distribution, and function. J. Clin. Sleep Med. **2**(2), 7–11 (2006)
59. Olsen, R.W., Sieghart, W.: International Union of Pharmacology. LXX. Subtypes of gamma-aminobutyric acid(A) receptors: classification on the basis of subunit composition, pharmacology, and function. Update. Pharmacol. Rev. **60**(3), 243–260 (2008)

60. Partadiredja, G., Miller, R., Oorschot, D.: The number, size, and type of axons in rat subcortical white matter on left and right sides: a stereological, ultrastructural study. J. Neurocytol. **32**, 1165–1179 (2003)
61. Pitot, M., Gastaut, H.: [Electroencephalographic modifications during the estrus cycle]. Rev. Neurol. (Paris) **89**(5), 427–430 (1953)
62. Reddy, D.S.: Neurosteroids: endogenous role in the human brain and therapeutic potentials. Prog. Brain Res. **186**, 113–137 (2010)
63. Regan, D.: Human Brain Electrophysiology: Evoked Potentials and Evoked Magnetic Fields in Science and Medicine. Elsevier, New York (1989)
64. Ritchie, J.: Physiology of axons. In: Waxman, S., Kocsis, J., Stys, P. (eds.) The Axon: Structure, Function and Pathophysiology, pp. 68–96. Oxford University Press, New York (1995)
65. Robinson, P., Rennie, C., Wright, J.: Propagation and stability of waves of electrical activity in the cerebral cortex. Phys. Rev. E **56**, 826–840 (1997)
66. Robinson, P.A., Rennie, C.J., Rowe, D.L., O'Connor, S.C.: Estimation of multiscale neurophysiologic parameters by electroencephalographic means. Hum. Brain Mapp. **23**(1), 53–72 (2004)
67. Rudolph, U., Antkowiak, B.: Molecular and neuronal substrates for general anaesthetics. Nat. Rev. Neurosci. **5**, 709–720 (2004)
68. Sherman, S., Guillery, R.: Exploring the thalamus and its role in cortical function. MIT, Cambridge (2005)
69. Sohl, G., Maxeiner, S., Willecke, K.: Expression and functions of neuronal gap junctions. Nat. Rev. Neurosci. **6**(3), 191–200 (2005)
70. Stam, C.: Nonlinear dynamical analysis of EEG and MEG: review of an emerging field. Clin. Neurophysiol. **116**, 2266–2301 (2005)
71. Stam, C., Pijn, J., Suffczyński, P., Lopes da Silva, P.: Dynamics of the human alpha rhythm: evidence for non-linearity? Clin. Neurophysiol. **110**, 1801–1813 (1999)
72. Steyn-Ross, D., Steyn-Ross, M., Sleigh, J., Wilson, M.: Progress in modelling EEG effects of general anesthesia: biphasic response and hysteresis. In: Hutt, A. (ed.) Sleep and Anesthesia: Neural Correlates in Theory and Experiment. Springer Series in Computational Neuroscience, pp. 167–94. Springer, New York (2011)
73. Stys, P.K.: The axo-myelinic synapse. Trends Neurosci. **34**(8), 393–400 (2011)
74. Terzuolo, C.A., Bullock, T.H.: Measurement of imposed voltage gradient adequate to modulate neuronal firing. Proc. Natl. Acad. Sci. U.S.A. **42**(9), 687–694 (1956)
75. van Veen, L., Liley, D.: Chaos via Shilnikov's saddle-node bifurcation in a theory of the electroencephalogram. Phys. Rev. Lett. **97**, 208101 (2006)
76. Wendling, F., Bartolomei, F., Bellanger, J.J., Chauvel, P.: Epileptic fast activity can be explained by a model of impaired GABAergic dendritic inhibition. Eur. J. Neurosci. **15**(9), 1499–1508 (2002)
77. Wilson, H., Cowan, J.: Excitatory and inhibitory interactions in localized populations of model neuron. Biophys. J. **12**, 1–24 (1972)
78. Wilson, H., Cowan, J.: A mathematical theory of the functional dynamics of cortical and thalamic nervous tissue. Kybernetik **13**, 55–80 (1973)